

# Slim accretion discs: a model for ADAF-SLE transitions

Igor V. Igumenshchev<sup>1,2\*</sup>, Marek A. Abramowicz<sup>1,3,4</sup> and Igor D. Novikov<sup>5,3,6,7</sup>

<sup>1</sup>*Department of Astronomy & Astrophysics, Göteborg University and Chalmers University of Technology, 412 96 Göteborg, Sweden*

<sup>2</sup>*Institute of Astronomy, 48 Pyatnitskaya Street, Moscow, 109117, Russia*

<sup>3</sup>*Nordita, Blegdamsvej 17, DK-2100 Copenhagen Ø, Denmark*

<sup>4</sup>*Laboratorio Interdisciplinare SISSA, Trieste, Italy, and ICTP, Trieste, Italy*

<sup>5</sup>*Theoretical Astrophysics Center, Juliane Maries Vej 30, DK-2100 Copenhagen Ø, Denmark*

<sup>6</sup>*University Observatory, Juliane Maries Vej 30, DK-2100 Copenhagen Ø, Denmark*

<sup>7</sup>*P. N. Lebedev Physical Institute, 84/32 Profsoyuznaya Street, Moscow, 117810, Russia*

Accepted 1997 September 00. Received 1997 September 00; in original form 1997 September 00

## ABSTRACT

We numerically construct slim, global, vertically integrated models of optically thin, transonic accretion discs around black holes, assuming a regularity condition at the sonic radius and boundary conditions at the outer radius of the disc and near the black hole. In agreement with several previous studies, we find two branches of shock-free solutions, in which the cooling is dominated either by advection, or by local radiation. We also confirm that the part of the accretion flow where advection dominates is in some circumstances limited in size: it does not extend beyond a certain outer limiting radius. New results found in our paper concern the location of the limiting radius and properties of the flow near to it. In particular, we find that beyond the limiting radius, the advective dominated solutions match on to Shapiro, Lightman & Eardley (SLE) discs through a smooth transition region. Therefore, the full global solutions are shock-free and unlimited in size. There is no need for postulating an extra physical effect (e.g. evaporation) for triggering the ADAF-SLE transition. It occurs due to standard accretion processes described by the classic slim disc equations.

**Key words:** accretion, accretion discs – hydrodynamics – relativity – methods: numerical.

## 1 INTRODUCTION

Most of our knowledge about accretion disc structure comes from a very successful, but simplified, approach introduced by Shakura (1972), Pringle & Rees (1972), Shakura & Sunyaev (1973) and others. In this approach, only the radial structure of the disc is studied in a detailed way, and all of the disc properties are taken to be independent of time and azimuthal angle and are averaged in the vertical direction. Let  $H = H(r)$  be the vertical extension of the disc at a particular radial location  $r$ . In the standard Shakura-Sunyaev ‘thin’ model, terms of the order  $(H/r)^2$  and higher are neglected. This allows the problem to be reduced to a set of linear algebraic equations which it is easy to solve: the standard model gives explicitly all of physical characteristics of the disc.

However, the  $(H/r)^2$  terms, which are neglected in the standard thin disc model, describe effects that in many as-

trophysical applications are very relevant: the radial pressure gradient, non-Keplerian angular momentum distribution, and cooling by radial advection of heat. These terms are all retained in the ‘slim’ accretion discs models introduced by Abramowicz et al. (1988, hereafter ACLS88) and based on a set of non-linear radial differential equations derived by Paczyński & Bisnovatyi-Kogan (1981). Mathematically, integrating the slim disc equations leads to a non-standard eigenvalue problem which is surprisingly difficult to solve. The original ACLS88 slim disc models, and slim models studied later by many other authors, have been constructed with a help of a very accurate pseudo-Newtonian model of the black hole gravitational field (Paczyński & Wita 1980). Lasota (1994) derived the full set of slim accretion disc equations in Kerr geometry, i.e. in the gravitational field of a rotating black hole. Abramowicz et al. (1996, hereafter ACGL96), and Abramowicz, Lanza & Percival (1997) later made some improvements and corrections to Lasota’s equations. Recently, Beloborodov, Abramowicz & Novikov (1997) rederived the relativistic slim accretion disc equations

\* E-mail: ivi@fy.chalmers.se

again, taking into account the relativistic effect of the heat inertia that is important for discs around rapidly rotating black holes, but was neglected by previous investigators.

Initially, all of the slim models were constructed under the assumption of the disc being very optically thick but a few years ago it was realized by Narayan & Yi (1994), Abramowicz et al. (1995), and Narayan & Yi (1995) that a new class of very hot, optically thin, advective discs exists. The new class are called ADAFs and are very promising for explaining properties of X-ray transients, low luminosity active galactic nuclei, the Galactic Centre, and other high energy objects. For this reason they are now being studied intensively by many researchers (see Narayan 1997, for a review and references).

The first ADAF models were local (in the sense that no boundary conditions were applied), and were constructed with many simplifying assumptions. Only very recently have several authors constructed more accurate, slim global models. Chen, Abramowicz & Lasota (1997), Narayan, Kato & Honma (1997), and Nakamura et al. (1997) constructed global transonic models for ADAFs using the Paczyński-Witta model for the black hole gravity. ACGL96 and Jaroszyński & Kurpiewski (1997) constructed global transonic ADAF models in Kerr geometry, using Lasota's equations.

In this paper we construct some new black hole models of slim discs, using Lasota's equations in the version given by ACGL96 and Abramowicz et al. (1997a), where the influence of the heat inertia (discussed in Beloborodov et al. 1997) was neglected. Equations, boundary conditions and the numerical procedure are presented in Section 2. In Section 3 we give the numerical results for adiabatic and non-adiabatic models. Section 4 contains the final discussion and conclusions. The new type of global transonic models found in our paper consist of an ADAF in the inner part and an SLE (Shapiro, Lightman & Eardley 1976) type of flow in the outer part. The SLE discs are known to be violently unstable (Piran 1978), and therefore our solutions with the ADAF-SLE transitions are not astrophysically realistic models of stationary accretion flows. However, they provide a non-trivial example of the ADAF-(thin disc) transition and for this reason they could be of interest.

## 2 METHOD OF SOLUTION

### 2.1 Equations

The equations for Keplerian discs in the Kerr metric were derived by Novikov & Thorne (1973). We follow the notation and equations in ACGL96 for non-Keplerian slim discs, except where explicitly indicated.

The mass conservation equation reads,

$$\dot{M} = -2\pi\Delta^{1/2}\Sigma\frac{V}{\sqrt{1-V^2}}, \quad (2.1)$$

where  $\Sigma = 2H\rho$  is the surface density,  $H$  is the half-thickness of the disc,  $\rho$  is the rest mass density at the equatorial plane and  $V$  is the radial velocity, defined later by the equation (2.16).

The equation of radial momentum conservation takes the form,

$$\frac{V}{\sqrt{1-V^2}}\frac{dV}{dr} = \frac{A}{r} - \frac{1}{\rho}\frac{dp}{dr}, \quad (2.2)$$

where the pressure  $p$  is at the equatorial plane, and

$$A = -\frac{MA}{r^3\Delta\Omega_K^+\Omega_K^-}\frac{(\Omega-\Omega_K^+)(\Omega-\Omega_K^-)}{1-\tilde{\Omega}^2\tilde{R}^2}. \quad (2.3)$$

The definitions of the symbols introduced above are given later in this Section. The last term in equation (2.2) differs from the one used by ACGL96.

The equation of angular momentum conservation,

$$\frac{\dot{M}}{2\pi r}\frac{d\mathcal{L}}{dr} + \frac{1}{r}\frac{d}{dr}\left(\Sigma\nu A^{3/2}\frac{\Delta^{1/2}\gamma^3}{r^4}\frac{d\Omega}{dr}\right) = 0, \quad (2.4)$$

where

$$\mathcal{L} = -u_\varphi = \gamma\left(\frac{A^{3/2}}{r^3\Delta^{1/2}}\right)\tilde{\Omega} \quad (2.5)$$

is the specific angular momentum.

The equation of energy conservation in the one temperature ( $T_e = T_i = T$ ) approximation,

$$\frac{\dot{M}}{2\pi r^2}\frac{p}{\rho}\left(\frac{1}{\gamma_g-1}\frac{d\ln T}{d\ln r} - \frac{d\ln\rho}{d\ln r}\right) = F^+ - F^-, \quad (2.6)$$

where  $\gamma_g$  is the adiabatic index of the gas,

$$F^+ = \nu\Sigma\frac{A^2}{r^6}\gamma^4\left(\frac{d\Omega}{dr}\right)^2 \quad (2.7)$$

is the surface heat generation rate, and  $F^-$  is the radiative cooling flux. For the case of proton-electron bremsstrahlung cooling, the emissivity per unit volume takes the form

$$\frac{F^-}{2H} = 5.6 \times 10^{20} \rho^2 T^{1/2} \text{ ergs cm}^{-3} \text{ s}^{-1}. \quad (2.8)$$

The equation (2.6) is written for a gas-pressure dominated medium with the equation of state

$$p = \frac{\mathcal{R}}{\mu}\rho T, \quad (2.9)$$

where  $\mathcal{R}$  is the gas constant,  $\mu$  is the mean molecular weight of gas ( $\mu = 1/2$  for a hydrogen plasma).

We take the equation of vertical balance in the form given by Abramowicz, Lanza & Percival (1997),

$$\frac{p}{\rho} = \frac{1}{2}\frac{u_\varphi^2 - u_t^2 a^2 + a^2}{r^2}\left(\frac{H}{r}\right)^2, \quad (2.10)$$

where

$$u_t^2 = \frac{\gamma^2 A}{r^2 \Delta} \left( \frac{r^2 \Delta}{A} + \frac{A}{r^2} \omega \tilde{\Omega} \right)^2 \quad \text{and} \quad u_\varphi^2 = \frac{\gamma^2 A}{r^2 \Delta} \frac{A^2}{r^4} \tilde{\Omega}^2. \quad (2.11)$$

In equations (2.1) – (2.11), we have used the following definitions,

$$\Delta = r^2 - 2Mr + a^2, \quad \omega = \frac{2Mar}{A}, \quad (2.12)$$

$$\tilde{R}^2 = \frac{A^2}{r^4 \Delta}, \quad A = r^4 + r^2 a^2 + 2Mra^2,$$

where  $M$  is the mass and  $a$  is the total specific angular momentum of the Kerr black hole.

$$\Omega = \frac{u^\varphi}{u^t} \quad \text{and} \quad \tilde{\Omega} = \Omega - \omega \quad (2.13)$$

are the angular velocities with respect to a stationary observer and to a local inertial observer,  $u^\varphi$  and  $u^t$  are components of the four-velocity  $u^i$  of matter. The angular frequencies of the corotating (+) and counterrotating (−) Keplerian orbits are

$$\Omega_K^+ = \frac{M^{1/2}}{r^{3/2} + aM^{1/2}}, \quad \Omega_K^- = -\frac{M^{1/2}}{r^{3/2} - aM^{1/2}}. \quad (2.14)$$

The relation between the Boyer-Lindquist and physical velocity components in the azimuthal direction is

$$v^{(\varphi)} = \tilde{R}\tilde{\Omega}. \quad (2.15)$$

The radial velocity  $V$  is defined by the formula

$$\frac{V}{\sqrt{1-V^2}} = u^r g_{rr}^{1/2}, \quad (2.16)$$

where  $g_{rr}$  is the metric tensor component. The velocity  $V$  is the radial velocity of the fluid as measured by an observer at fixed  $r$  who corotates with the fluid. The Lorentz gamma factor can be written as

$$\gamma^2 = \left( \frac{1}{1 - (v^{(\varphi)})^2} \right) \left( \frac{1}{1 - V^2} \right). \quad (2.17)$$

We use the standard assumption for the viscosity coefficient,

$$\nu = \alpha c_s H, \quad (2.18)$$

where  $\alpha$  is a parameter and  $c_s = (p/\rho)^{1/2}$  is the isothermal sound speed.

## 2.2 Conditions at the sonic radius

The differential equations (2.2) and (2.6) can be rewritten in a form where just two unknown functions  $V(r)$ , and  $T(r)$  are present,

$$\frac{d \ln V}{d \ln r} = (1 - V^2) \frac{N}{D}, \quad (2.19)$$

$$\frac{d \ln T}{d \ln r} = -\frac{\gamma_g - 1}{\gamma_g + 1} \left\{ 2(1 - \eta V^2) \frac{N}{D} + \frac{4\pi r^2}{M c_s^2} (F^+ - F^-) + \mathcal{B} \right\}, \quad (2.20)$$

where

$$N = \mathcal{A} + \frac{2\pi r^2}{M} \frac{\gamma_g - 1}{\gamma_g + 1} (F^+ - F^-) + \frac{\gamma_g}{\gamma_g + 1} c_s^2 \mathcal{B}, \quad (2.21)$$

$$D = V^2 \left( 1 + \frac{2\gamma_g}{\gamma_g + 1} \eta c_s^2 \right) - \frac{2\gamma_g}{\gamma_g + 1} c_s^2, \quad (2.22)$$

$\mathcal{A}$  is defined by equation (2.3) and

$$\mathcal{B} = 4 + 2 \frac{r(r-M)}{\Delta} - \eta \left( \frac{2(v^{(\varphi)})^2}{1 - (v^{(\varphi)})^2} \frac{d \ln v^{(\varphi)}}{d \ln r} + \frac{d \ln \Psi}{d \ln r} \right),$$

$$\Psi = (1 - a^2 \omega^2) \frac{A}{r^2 (v^{(\varphi)})^2} - 2a^2 \Delta^{1/2} \omega v^{(\varphi)} - a^2 \frac{r^2 \Delta}{A},$$

$$\eta = \left( 1 + \frac{a^2}{\Psi \gamma^2} \right)^{-1}.$$

The regularity condition at the critical point  $r_s$  of equations (2.19) and (2.20) requires that

$$N|_{r_s} = 0, \quad D|_{r_s} = 0, \quad (2.23)$$

where  $N$  and  $D$  are given by the expressions (2.21) and (2.22). In the nonrelativistic limit, the condition  $D = 0$  reduces to  $V^2 = 2\gamma_g c_s^2 / (\gamma_g + 1)$ . We note that in our version of the vertically integrated equations, the velocity at the critical point does not coincide with the adiabatic sound speed, as it does in the case of the spherical accretion (Bondi 1954). Nevertheless, following tradition, we use the name the ‘sonic radius’ for the critical point  $r_s$ , and define the Mach number as

$$\mathcal{M} = \left( \frac{\gamma_g + 1}{2\gamma_g} + \eta c_s^2 \right)^{1/2} \frac{V}{c_s}. \quad (2.24)$$

## 2.3 Boundary conditions

The set of equations to be solved consists of two first order differential equations (2.2) and (2.6), and one second order equation (2.4). To find a solution with given  $\dot{M}$ ,  $\alpha$  and  $M$ , four integration constants (free parameters) are required, but the regularity condition (2.23) at the sonic radius reduces the number of free parameters in the problem to three. The choice of the three free parameters should be determined by fixing the boundary conditions. This may be done in many ways, but only certain particular choices will be consistent with stable numerical algorithms.

The standard approach is to fix boundary conditions at a large distance from the central accreting black hole (e.g. ACLS88, Chen et al. 1997) but a modification of this was used by Narayan et al. (1997) who specified  $\Omega = \Omega_K$  and  $c_s = 10^{-3} \Omega r$  at the outer boundary and the no-torque condition  $d\Omega/dr = 0$  at the inner boundary located between the black hole horizon and the sonic radius. It is well known that when the standard (or modified standard) boundary conditions are used, the mathematical problem is an eigenvalue problem that is numerically very time consuming and difficult to solve.

To avoid this difficulty, Chakrabarti and his collaborators (see Chakrabarti 1996 for references) introduced a very clever mathematical trick. They assumed a different set of boundary conditions, which are applied not only at the outer boundary, but also at the sonic radius and near to the black hole horizon. In this way, the most difficult part of the problem – finding the eigenvalue – is trivially solved: the eigenvalue may be assumed to have any particular value (in practice from some continuous range) and the outer boundary conditions automatically follow from it. In a way, this is putting the cart before the horse: one tries to match a problem to an already known solution. While this is obviously a perfectly acceptable mathematical procedure, there is no guarantee that solutions constructed in this way will always be astrophysically acceptable. One should worry about the appearance of unphysical discontinuities which prevent solutions extending smoothly out to very large radii. Troubled solutions such as these may correspond to *incorrect* choices of eigenvalues in the sense that no astrophysically acceptable outer boundary conditions are consistent with them.

In order to see how qualitative differences in the treatment of the boundary conditions influence numerical models of global transonic solutions describing slim accretion discs, we have adopted in this paper a procedure that is very similar to the one used by Chakrabarti and collaborators. Specifically, we take the position of the sonic radius  $r_s$  as one of

the free parameters. The second free parameter is fixed by the condition that the angular momentum tends asymptotically to a constant value near to the black hole horizon  $r_h$ . We assume that at the inner boundary  $r_{in}$  of the disc, the radial change of angular momentum is already negligible,

$$\left. \frac{d\mathcal{L}}{dr} \right|_{r_{in}} = 0. \quad (2.25)$$

Strictly speaking, in (2.25) one should set  $r_{in} = r_h$ . In practice, however, in numerical calculations one may choose the location of the inner boundary to be anywhere between the horizon and the sonic point, and the results change only slightly. We use  $r_{in} = (r_h + r_s)/2$  in our numerical calculations.

The third parameter is specified at the outer boundary  $r_{out}$ , by fixing the angular velocity,

$$\Omega(r_{out}) = \Omega_{out}, \quad (2.26)$$

as a fraction of the Keplerian angular velocity  $\Omega_K(r_{out})$ .

## 2.4 Numerical procedure

The set of nonlinear differential equations (2.4), (2.19) and (2.20) are solved numerically on a fixed numerical grid by means of a standard relaxation technique. This determines the solution by starting from an initial estimate which is then improved iteratively. The original differential equations are replaced by approximate finite-difference equations. We used two overlapping grids, one of which,  $\{r_i\}$ ,  $i = 1, \dots, N$ , is used for the second-order equation (2.4) while the other,  $\{r_{i+1/2}\}$ ,  $i = 1, \dots, N - 1$ , is used for equations (2.19) and (2.20). Variables  $\Omega_i$ ,  $i = 1, \dots, N$ , and  $V_{i+1/2}$ ,  $T_{i+1/2}$ ,  $i = 1, \dots, N - 1$ , are defined on grids  $\{r_i\}$  and  $\{r_{i+1/2}\}$ , respectively. It is assumed that the position of the sonic point  $r_s$  coincides with one of the points  $r_{i+1/2}$  at  $i = N_s$ .

The problem involves  $3N - 6$  coupled finite-difference (algebraical) equations which depend on  $3N - 2$  variables. This set of equations can be uniquely solved if we exclude two variables  $\Omega_1$  and  $\Omega_N$  using the conditions (2.25) and (2.26), respectively, and another two variables  $V_{N_s+1/2}$  and  $T_{N_s+1/2}$  using the conditions (2.23) at the sonic radius. Then, the system of  $3N - 6$  algebraical equations

$$F_k(x_1, x_2, \dots, x_{3N-6}) = 0 \quad k = 1, 2, \dots, 3N - 6, \quad (2.27)$$

where

$$x_k = \begin{pmatrix} \Omega_2, \dots, \Omega_{N-1}, V_{3/2}, \dots, V_{N_s-1/2}, \\ V_{N_s+3/2}, \dots, V_{N-1/2}, T_{3/2}, \dots, T_{N_s-1/2}, \\ T_{N_s+3/2}, \dots, T_{N-1/2} \end{pmatrix},$$

is solved by means of a multidimensional Newton iteration method (see, for example, Press et al. 1992). In matrix notation, the procedure of solution for equations  $\mathbf{F}(\mathbf{x}) = 0$  can be represented as,

$$\mathbf{x}_{new} = \mathbf{x}_{old} + \varepsilon \cdot \delta \mathbf{x}, \quad 0 < \varepsilon \leq 1, \quad (2.28)$$

where

$$\delta \mathbf{x} = -\mathbf{J} \cdot \mathbf{F}. \quad (2.29)$$

Here  $\mathbf{J}$  is the Jacobian matrix,  $J_{ij} \equiv \partial F_i / \partial x_j$ . We take a value of the parameter  $\varepsilon$  less than 1 to obtain convergence if the initial guess is not sufficiently close to the solution but then, when  $\mathbf{x}$  becomes close to the solution, we use the full

Newton step,  $\varepsilon = 1$ , to obtain the fastest (quadratic) convergence. Finally, we check the degree to which both functions and variables have converged.

## 3 RESULTS

We have constructed two families of models: a family of *adiabatic models* in which radiative cooling was neglected and a family of *bremstrahlung models* with bremsstrahlung cooling. In both cases we assumed a Schwarzschild black hole, with  $a = 0$ , and took the disc matter to consist of hydrogen plasma with  $\mu = 1/2$ . We used two values for the adiabatic index in the models,  $\gamma_g = 5/3$ ,  $4/3$ , the first corresponding to gas pressure domination while the second could represent the case where isotropically tangled magnetic field provides a major contribution to the total pressure. It is often argued that in realistic astrophysical accretion flows, the gas and magnetic pressures are roughly the same. Thus, one may assume that the effective adiabatic index has a value between  $4/3$  and  $5/3$ .

### 3.1 Adiabatic models

We take  $F^- = 0$  in equation (2.6) in order to study the pure effect of advection dominated cooling. For a given value of  $\gamma_g$ , there are two main parameters of models:  $\alpha$  and  $r_s$ . Solutions depend only very weakly on other parameters (see Section 2.3). In particular, the problem is independent of the mass  $M$  after a radial re-scaling with  $r_g = 2GM/c^2$ .

We now describe models with adiabatic index  $\gamma_g = 5/3$ . Two types of numerical solution have been found in this case. The first type, which are limited in size, can be constructed if  $r_s > (r_s)_{crit}$ , where  $(r_s)_{crit}$  depends on  $\alpha$ . They cannot extend in the radial direction beyond a radius  $r_{out}^{max}$  at which the thickness  $H$  goes to zero; it is impossible to construct models with  $r_{out}$  larger than this. The value of  $r_{out}^{max}$  is a decreasing function of  $r_s$ . Our numerical procedure can find only an approximate value for  $r_{out}^{max}$ , because  $dH/dr$  becomes singular ( $dH/dr \rightarrow -\infty$ ) when  $H \rightarrow 0$ , but one can set the outer boundary condition at  $r_{out} < r_{out}^{max}$  and obtain solutions which are just part of the solution with  $r_{out} = r_{out}^{max}$ . All of these models have the ratio  $H/r$  less than one everywhere, and so the condition for the slim disc approach to be self-consistent ( $H/r \lesssim 1$ ) is satisfied. Models with  $r_s = (r_s)_{crit}$  have the maximal value of  $H/r$  approximately equal to one. Models of this type can experience a transition at radius  $\approx r_{out}^{max}$  to a thin disc of the type allowed by the energy equation. In Section 3.2, an example of the transition of an ADAF to an SLE-type disc is given.

The second type of solution exists when  $r_s < (r_s)_{crit}$ . Models of this type are not size-limited in the radial direction; indeed, their properties depend strongly on the value of  $r_{out}$ . In particular, the maximum value of the ratio  $H/r$  is an increasing function of  $r_{out}$ . Typically, these models have  $H/r \gg 1$  for the whole range of radii,  $r_{in} < r < r_{out}$  (models with  $H/r < 1$  everywhere exist only for a small value of  $r_{out}$ ). This type of solution is not self-consistent because it does not satisfy the slim disc condition for large  $r$  and so we will not discuss it further. In the following, we will only discuss models of the first type, which have limited radial size.

**Table 1.** Parameters of the adiabatic accretion disc models (adiabatic index  $\gamma_g = 5/3$ ). The radial distances  $r_s$ ,  $(r_s)_{crit}$ ,  $r_{out}^{max}$  are given in units of the gravitational radius  $r_g$ .

Model	$\alpha$	$r_s$	$(r_s)_{crit}$	$r_{out}^{max}$
A1	0.1	2.485	2.485	24.0
A2		2.5		16.8
A3		2.55		11.1
B1	0.01	2.165	2.165	85.7
B2		2.175		53.3
B3		2.2		29.0
B4		2.25		17.1
B5		2.3		13.0
C1	0.001	2.09	2.09	148.0
C2		2.1		73.0
C3		2.125		37.4
C4		2.15		25.5
C5		2.2		15.7
D1	$10^{-5}$	2.05	2.05	245.0
D2		2.1		35.6
D3		2.15		18.6

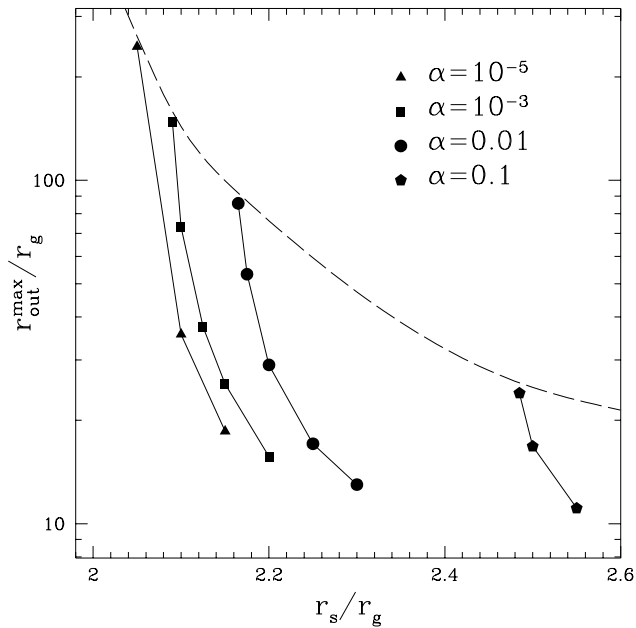


**Figure 1.** The dependence of maximal radial extension  $r_{out}^{max}$  of the adiabatic accretion disc models (adiabatic index  $\gamma_g = 5/3$ ) on the position of the transonic radius  $r_s$ . The data are shown for the viscosity parameter  $\alpha = 10^{-5}$ ,  $10^{-3}$ , 0.01 and 0.1 (triangles, squares, circles and pentagons, respectively). In the region above the dashed line, slim disc solutions do not exist.

Table 1 summarizes the basic parameters of the computed models with  $\alpha = 10^{-5}$ ,  $10^{-3}$ , 0.01 and 0.1. In these models  $r_{out}$  was set approximately equal to  $r_{out}^{max}$ . Fig. 1 shows the dependence of  $r_{out}^{max}$  on the position of the sonic radius for the solutions listed in Table 1, with the dashed line showing roughly the boundary of the region in the  $(r_s, r_{out}^{max})$  space where solutions of the first type exist. More extended discs correspond to smaller  $\alpha$  and smaller  $r_s$ . Fig. 2 shows the disc shapes  $H(r)$  for the largest discs (with  $r_s = (r_s)_{crit}$ )

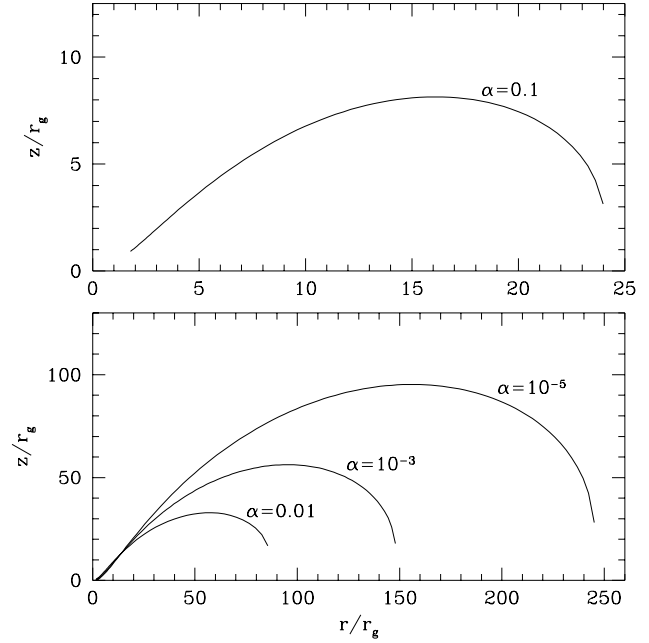


**Figure 2.** The shapes of the adiabatic accretion discs ( $\gamma_g = 5/3$ ) for four values of the viscosity parameter  $\alpha = 0.1$ , 0.01,  $10^{-3}$  and  $10^{-5}$ . The models presented have the maximal radial extensions for the given  $\alpha$ , and correspond to the models A1, B1, C1 and D1, listed in Table 1.

for the values of  $\alpha$  listed above (models A1, B1, C1 and D1). The shapes of these discs are very similar: the maximum vertical thickness occurs at around  $0.65r_{out}^{max}$  and the outer edge is very sharp. Figs 3, 4, and 5 show the variation with  $r$  of the angular momentum  $\mathcal{L}$ , the radial velocity  $V$  and the equatorial pressure  $p$ , for solutions with different values of  $\alpha$  and  $r_s$  (corresponding to the models listed in Table 1).

At the outer edge, all of the models have low values of  $V$  and  $c_s$ , and the distribution of angular momentum has a super-Keplerian part. The super-Keplerian rotation corresponds to a region where the pressure increases with radius (see Fig. 5). The pressure increases due to the rapid decrease of the disc thickness  $H$  at the outer boundary and the corresponding increase in the matter density. The super-Keplerian rotation compensates the gravitational force and the gradient in the gas pressure, which are both directed inwards in this region. The presence of super-Keplerian rotation does not depend on the particular value taken for  $\Omega_{out}$ . We tried a variety of values, both Keplerian and non-Keplerian, but always found the presence of super-Keplerian rotation. Note, that the super-Keplerian rotation often occurs in a region where a sharp transition in qualitative properties of the accretion flow takes place: the two sub-Keplerian flows on either side of the super-Keplerian part are very different. For example, super-Keplerian rotation occurs at the sharp, cusp-like inner edge of thick discs (Abramowicz, Calvani & Nobili 1980). In this case, the super-Keplerian part is sandwiched between supersonic free-fall with negligible dissipation, and centrifugally supported, viscously driven accretion flow. Super-Keplerian rotation is also expected in the transition region between a standard Shakura & Sunyaev disc and an ADAF (Abramowicz, Igumenshchev & Lasota 1997). We also note that the existence of super-Keplerian ro-

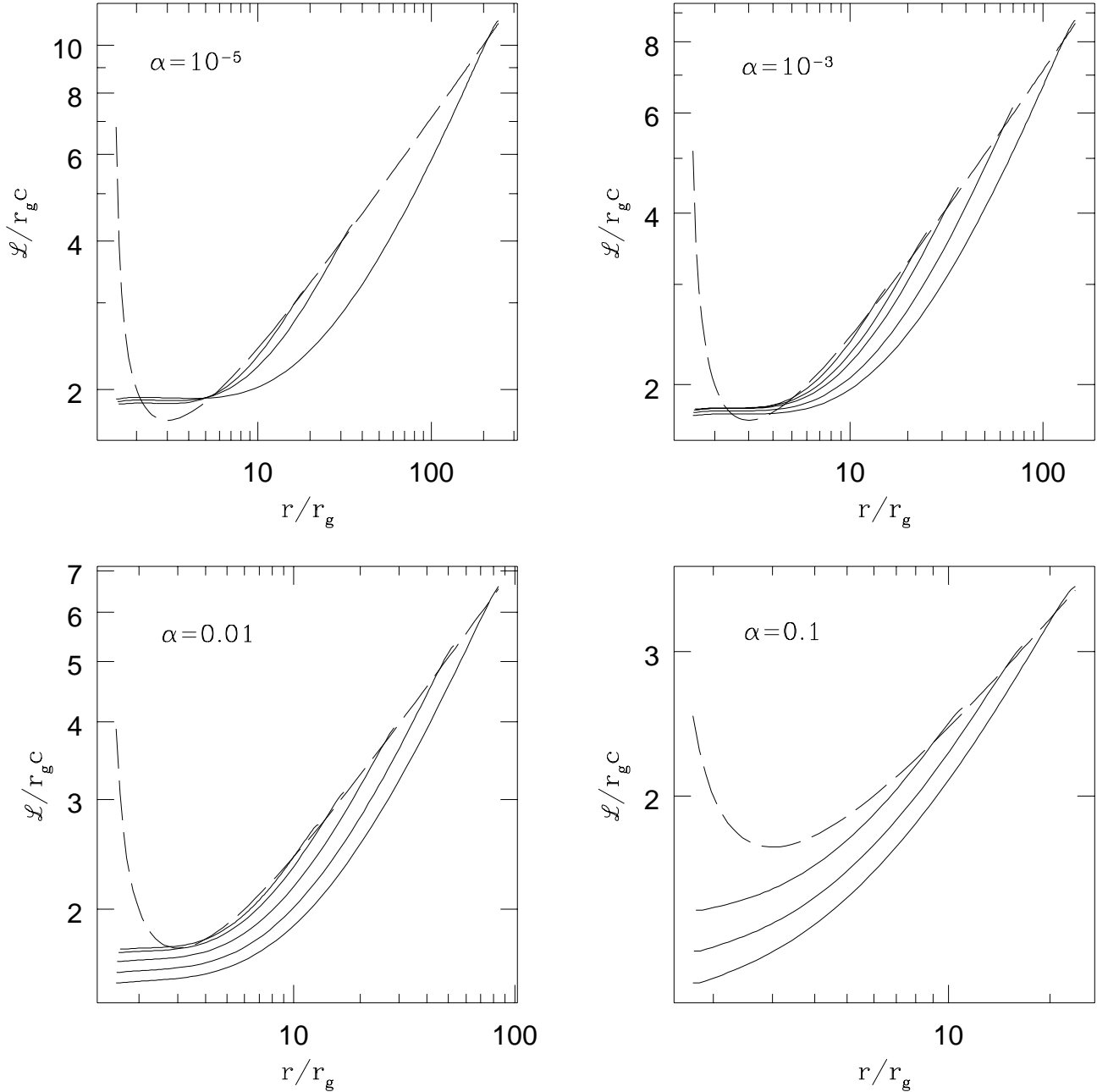


**Figure 3.** Distributions of angular momentum in the adiabatic models ( $\gamma_g = 5/3$ ) for four values of  $\alpha$  (solid lines). The distribution of the Keplerian angular momentum is shown for comparison (dashed lines). For each  $\alpha$ , the models have the values of the sonic radius  $r_s$  and the radial extension  $r_{out} = r_{out}^{max}$  given in Table 1.

tation at the outer edge of some ADAF models can be seen in a few solutions previously obtained by Honma (1996).

Just inside the outer boundary, the distribution of angular momentum  $\mathcal{L}$  is almost a power law with  $d \ln \mathcal{L} / d \ln r \approx 0.77$ , larger than the Keplerian value of 0.5 (see Fig. 3). We note, that this value is practically independent of  $\alpha$  and depends only weakly on  $r_s$ , if  $r_{out}^{max} \gtrsim 10r_g$ . In this case, the rotational energy of the accretion flow at the outer radii is being converted more efficiently into internal energy than in the case of a standard thin disc. As a result, both the temperature and the thickness of the disc increase rapidly inwards. A significantly sub-Keplerian rotation of this part

of the disc implies that the radial pressure gradient becomes important in the balance of radial forces.

Near to the black hole, solutions with high (super-Keplerian) and low (sub-Keplerian) angular momenta show qualitatively different behaviour. This was first noticed long ago by Abramowicz & Zurek (1981). When the boundary conditions are held fixed, high and low values of the angular momentum near to the black hole correspond to solutions with small and large values of  $\alpha$  respectively. These two types of solution were referred to as ‘disc-like’ and ‘Bondi-like’, respectively. Differences between the disc-like and Bondi-like solutions in the special case of very

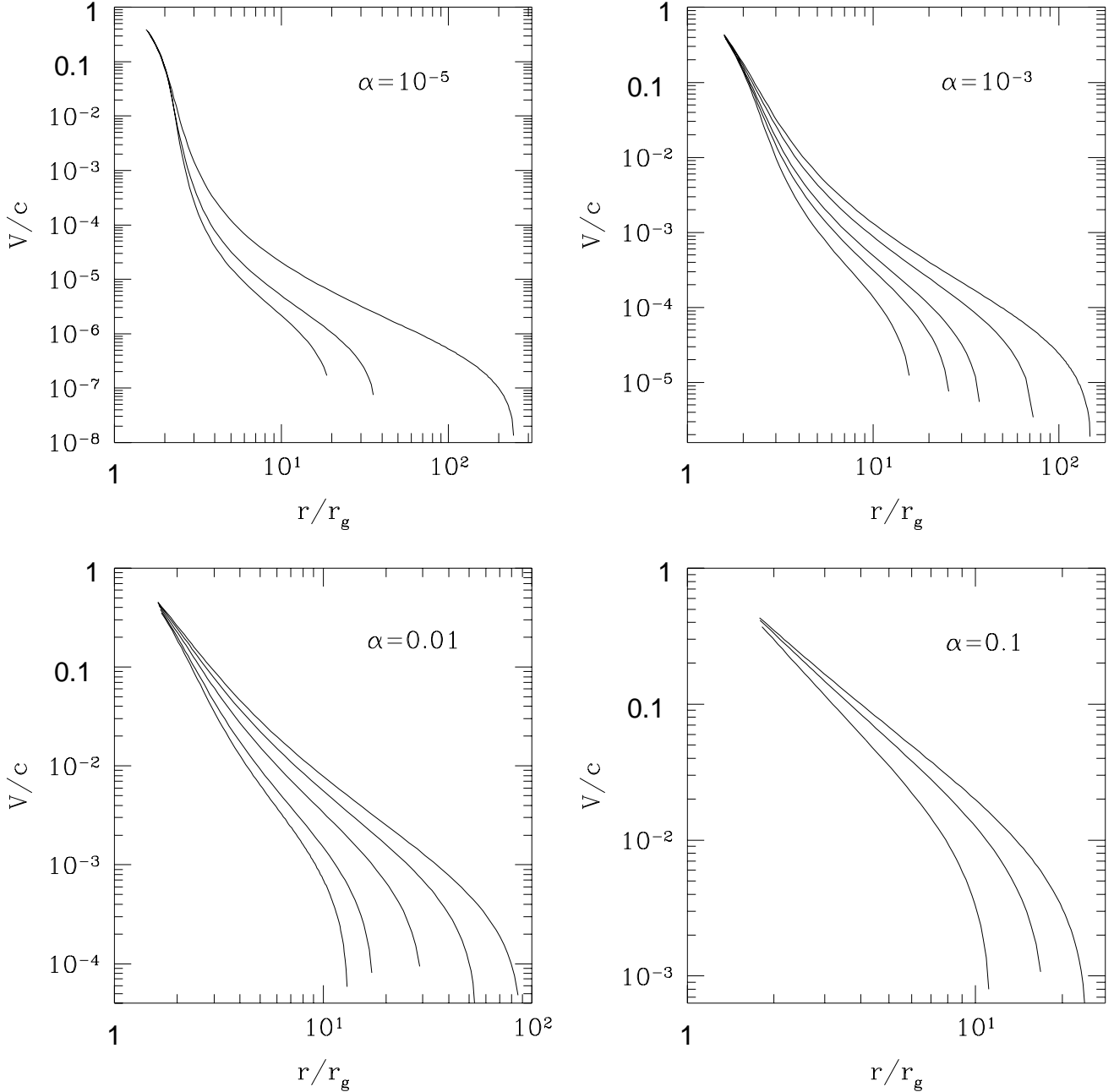


**Figure 4.** Distributions of radial velocity in the adiabatic models with  $\gamma_g = 5/3$  (see the caption to Fig. 3 for further explanation).

geometrically-thin accretion flows have been discussed by Muchotrzeb (1983), and later by several other authors, including Matsumoto et al. (1984), ACLS88 and Narayan et al. (1997). Our results show the existence of disc-like and Bondi-like solutions in agreement with the general results of Abramowicz & Zurek (1981). In particular, we confirm a more recent specific example of this general property, found by Narayan et al. (1997) in the special case of ADAFs: for  $\alpha \lesssim 0.01$ , solutions are of the disc-like type, while for  $\alpha \gtrsim 0.01$  they are Bondi-like. For the disc-like solutions with small  $\alpha$ , the sonic radius is located near to the marginally-bound radius,  $2r_g < r_s \lesssim 2.3r_g$ , and the distribution of angular momentum has a super-Keplerian part around the marginally-stable radius (see Figs 1 and 3). For the Bondi-

like type, corresponding to large  $\alpha$ , the sonic radius is located closer to  $r_{ms}$ , and the angular momentum is substantially sub-Keplerian everywhere in the region. Note, that our Bondi-like solutions have  $r_s < r_{ms}$ . We did not find solutions with  $r_s > r_{ms}$  in case of  $\alpha \leq 0.1$ . The existence of solutions with  $r_s \gtrsim r_{ms}$  is questionable because the maximum radius of the disc  $r_{out}^{max}$  decreases quickly with increasing sonic radius for any  $\alpha$  (see Fig. 1).

Differences between these two classes of solution can also be seen in the radial distribution of the pressure. Disc-like models have pressure maxima outside the transonic point while these maxima disappear in Bondi-like models (see Fig. 5).

Models with adiabatic index  $\gamma_g = 4/3$  only have properties which are qualitatively similar to those with  $\gamma_g = 5/3$

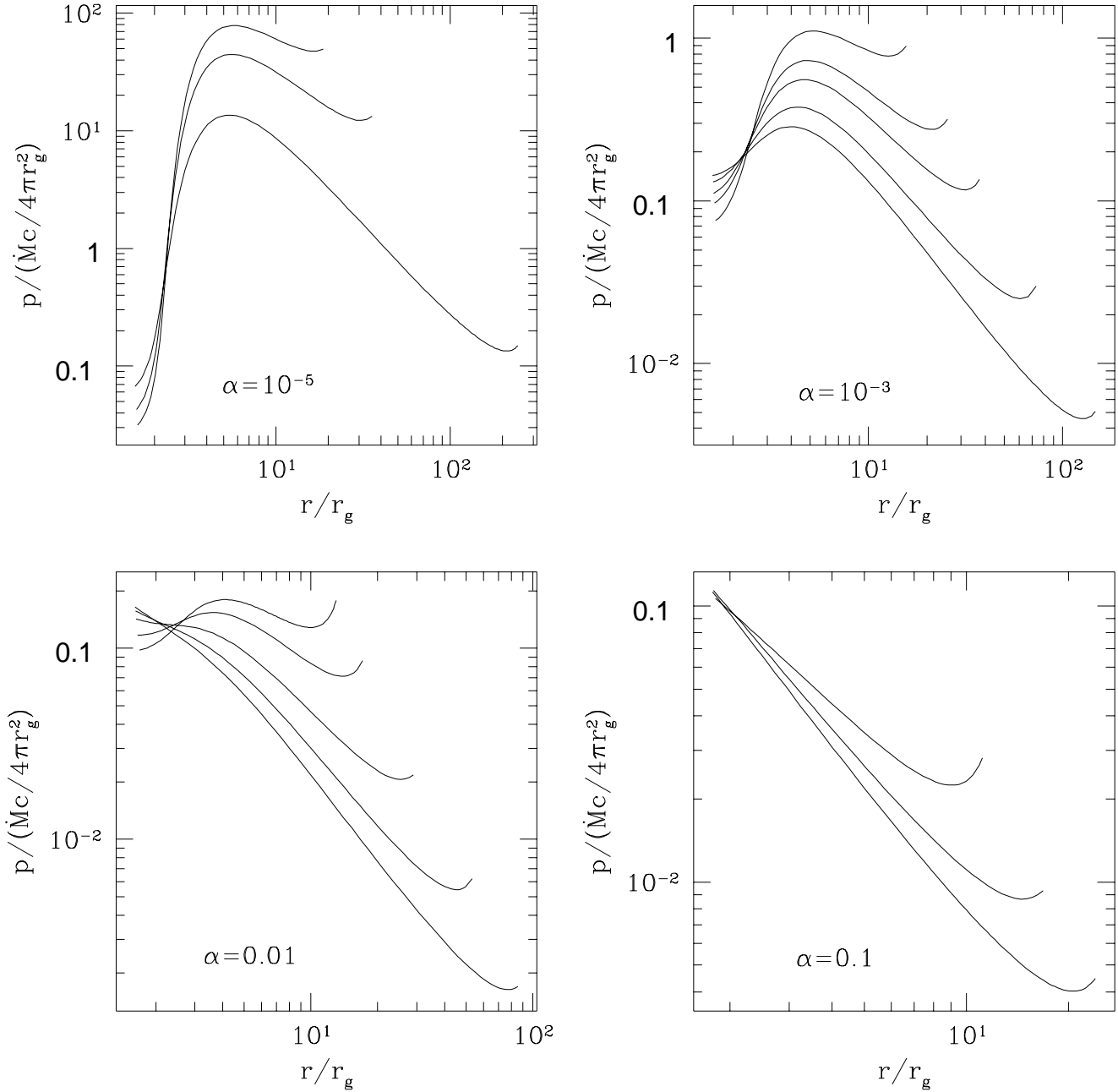


**Figure 5.** Distributions of pressure in the adiabatic models with  $\gamma_g = 5/3$  (see the caption to Fig. 3 for further explanation).

if the viscosity is high ( $\alpha \gtrsim 0.01$ ). In particular, all of our high viscosity models with  $H/r < 1$  and  $\gamma_g = 4/3$  are limited in size. It could be, however, that there are also models which are unlimited in size but which our numerical procedure was unable to find: for purely technical reasons, it does not converge well for highly viscous models with large  $r_{out}$ .

Models with  $\alpha \lesssim 0.001$  show a very different behaviour, however. Models with a particular value of the sonic radius,  $r_s = (r_s)_0$  are not limited in size and coincide asymptotically (for large radii) with the corresponding self-similar solutions of Narayan & Yi (1995). Models with  $r_s > (r_s)_0$  are limited in size with  $r_{out}^{max}$  being a decreasing function of  $r_s$ . For  $r_s < (r_s)_0$  the solutions have  $H/r > 1$  in the outer part and so do not satisfy the condition for the slim disc approximation.

### 3.2 Bremsstrahlung models

We now describe models with bremsstrahlung cooling, in particular, ones in which the inner ADAFs are matched with outer SLE type solutions. In the original SLE paper, ions and electrons were allowed to have different temperatures, and the assumption of equality of the local electron heating and cooling rates was used. We use a one-temperature approximation for plasma but, nevertheless, our bremsstrahlung solutions in the outer part can be treated as being of SLE type in the sense that they are locally cooled, i.e.  $F^+ \approx F^-$ .

Fig. 6 shows the radial dependence of the relative thickness  $H/r$ , the importance of the advective flux  $(F^+ - F^-)/F^+$ , the angular momentum  $\mathcal{L}$ , the equatorial pressure  $p$ , the Mach number  $\mathcal{M}$ , as defined by equation (2.24),



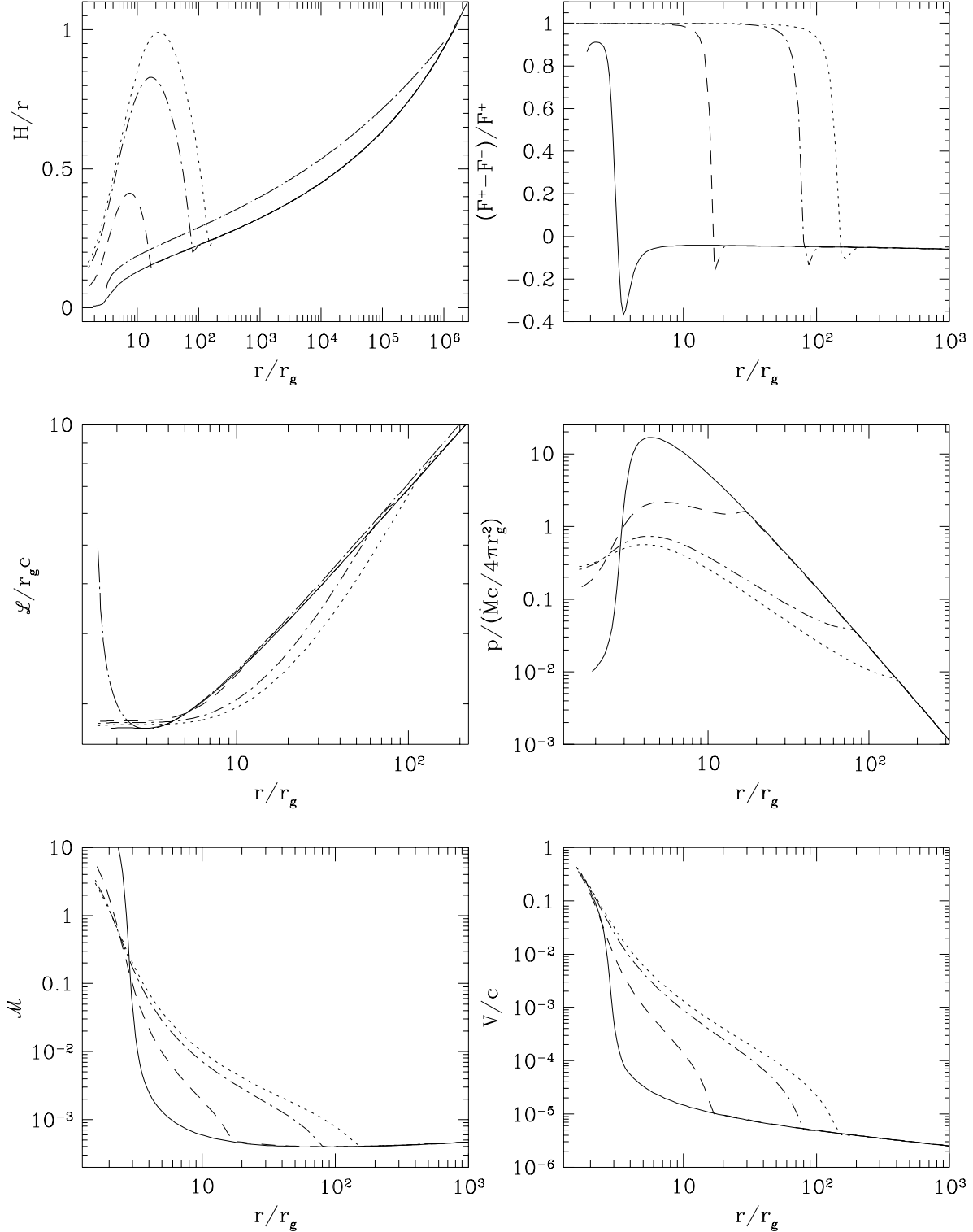


**Figure 6.** Selected properties of the bremsstrahlung models with  $\gamma_g = 5/3$ ,  $\alpha = 10^{-3}$ ,  $\dot{M}/\dot{M}_{Edd} = 10^{-5}$  and  $M = 10 M_\odot$ . The dotted, dotted-short-dashed, short-dashed and solid lines represent the cases  $r_s/r_g = 2.09, 2.1, 2.2$  and  $2.7$ , respectively. The behaviour of the analytic SLE solution (3.1) is shown for comparison by a dotted-long-dashed line in the aspect ratio  $H/r$  plot. A dotted-long-dashed line in the specific angular momentum  $\mathcal{L}/r_g c$  plot shows the Keplerian angular momentum distribution. The bottom left frame shows the run of the Mach number  $\mathcal{M}$  as defined by equation (2.24). The global solutions consist of two different parts with a relatively narrow transition region. At small  $r$ , the solutions behave like ADAFs, while at large  $r$  they behave like one-temperature SLE solutions. The model with  $r_s/r_g = 2.7$  (solid line) has special properties: it consists of the SLE solution everywhere except for the region inside  $3r_g$ .

and the velocity  $V$  for models with  $\gamma_g = 5/3$ ,  $\alpha = 10^{-3}$  and  $\dot{M}/\dot{M}_{Edd} = 10^{-5}$ . Here  $\dot{M}_{Edd} = 4\pi GMm_p/c\sigma_T$  is the Eddington accretion rate. The black hole mass was taken to be  $M = 10M_\odot$ . In these models we varied the position of the sonic radius. Dotted, dotted-short-dashed, short-dashed and solid lines represent the cases  $r_s/r_g = 2.09, 2.1, 2.2$  and  $2.7$ , respectively. Inward of the transition radius, the solutions become ADAFs with  $(F^+ - F^-)/F^+ \simeq 1$ , and they have all of the properties of the adiabatic models discussed in the previous paragraph. The transition radius between the two types of solution depends on  $r_s$ . This dependence, as well as the limitations of the minimum value of  $r_s$ , are very similar to those for  $r_{out}^{max}$  (see Fig. 1, square dots) and  $(r_s)_{crit}$  in adiabatic models. The model with  $r_s/r_g = 2.7$  (solid lines in Fig. 6) has special properties, because it becomes an ADAF just inside  $3r_g$ , and the transition radius is very close to the sonic radius.

Outside the transition radius, each solution matches smoothly with an SLE type solution, which is unique for given  $\alpha$ ,  $\dot{M}$  and  $M$ , and does not depend on the position of the transonic point  $r_s$  or the location of the transition radius. Note that we have not assumed any extra physical effect that triggers the transition. The transition occurs due to the standard accretion processes, described by the standard equations for slim accretion discs.

Of course, one may construct SLE solution analytically, taking  $\Omega = \Omega_K$ ,  $F^+ = F^-$  and zero viscous torque at  $r = 3r_g$ ,

$$\frac{H}{r} = 0.1 \left( \frac{\dot{m}}{\alpha^2} \right)^{1/4} \left( 1 - \sqrt{\frac{3r_g}{r}} \right)^{1/4} \left( \frac{r}{r_g} \right)^{1/8}, \quad (3.1)$$

where  $\dot{m} = \dot{M}/\dot{M}_{Edd}$ . The analytic SLE solution (3.1) is shown in Fig. 6 by the dotted-long-dashed line. There is good agreement between the analytic solution (3.1) and the numerical solution outside the transition radius. Both solutions have similar slopes inside  $\sim 10^5 r_g$ . Fig. 6 shows that the SLE type solutions have negative  $(F^+ - F^-)/F^+$  (see the discussion by Abramowicz 1996). In the standard SLE solution  $F^+ = F^-$ .

In Fig. 7 we show properties of the  $\gamma_g = 4/3$  models. Short-dashed, dotted, long-dashed, dotted-short-dashed and solid lines represent the cases  $r_s/r_g = 2.13075, 2.131, 2.14, 2.255$  and  $2.7$ , respectively. All of the models experience the ADAF-SLE transition. Note, that in models corresponding to the short-dashed and dotted lines, the ADAF part is very extended. In contrast to the previous ( $\gamma_g = 5/3$ ) case, we found an unphysical behaviour of the solutions for  $r > 10^5 r_g$ . In this radial range, the solutions have the angular momentum  $\mathcal{L}$  decreasing outwards, which is dynamically unstable. They also deviate strongly from the thermal structure characteristic of the SLE solution, having the cooling rate  $F^-$  significantly larger than the heating rate  $F^+$ . This behaviour does not depend either on the choice of the location of the outer numerical boundary  $r_{out}$ , or on the value taken for  $\Omega_{out}$ .

#### 4 DISCUSSION AND CONCLUSIONS

We have constructed numerical solutions for two classes of models of optically thin accretion discs around black holes:

adiabatic models, with no radiative cooling, and models with bremsstrahlung cooling.

All of the adiabatic models are of the ADAF type. Those with  $\gamma_g = 5/3$  and  $H/r \lesssim 1$  everywhere are limited in size: their radial extensions are smaller than about  $10^2 r_g$ . Independently of whether viscosity is high or low, the vertical thickness  $H$  of these models tends to zero at the outer limiting radius. Models with  $\gamma_g = 4/3$  and  $H/r \lesssim 1$  extend to radial infinity *only* when the viscosity is low (we constructed models with  $\alpha \lesssim 10^{-3}$ ) and when the location of the sonic point has exactly a particular value  $r_s = (r_s)_0$ . Obviously, this is the eigenvalue of the problem. It is therefore not surprising that these models have, at large distances, the same properties as the models corresponding to the self-similar solution of Narayan & Yi (1995). For  $r_s > (r_s)_0$  our models are radially limited. For discs with high viscosity ( $\alpha \gtrsim 10^{-2}$ ) we could not find disc-like solutions with unlimited radial size having  $H/r \lesssim 1$  everywhere. We cannot conclude that such solutions do not exist, due to numerical problems which our code experiences in this case. Radially unlimited solutions that we found in this range of parameters, all have the maximum value of  $H/r$  being an increasing function of the location taken for the outer numerical boundary  $r_{out}$ . In particular, for large  $r_{out}$  one always has  $H/r \gg 1$ . This indicates that the one-dimensional approach based on vertical integration which assumes  $H/r \lesssim 1$  is not self-consistent and slim models for this type of disc cannot be trusted.

Bremsstrahlung models consist of two parts which are joined by a smooth transition region. In some cases the transition region is relatively narrow (models with  $\gamma_g = 5/3$ ), but in other cases it can be larger than the ADAF. Inside the transition radius, the solution is very similar to the ADAF-type adiabatic solution. Outside it, the solution is of the SLE type, with the entropy of the matter increasing with radius. Our numerical SLE-type solutions coincide closely with the analytical ones. Obviously, though, this kind of global solution cannot exist in nature, because the outer SLE-type disc is thermally unstable.

The most interesting property of the ADAF solutions found in this paper is their behaviour near to the transition radius. It was known previously (see e.g. discussion given by Chen et al. 1995) that the ADAF-type accretion flows cannot extend to arbitrarily large radii — they may extend out to  $\sim 10^6 r_g$ . The limitation is due to the fact that at large radii the accretion time scale exceeds the free-free cooling time. This case is represented by the model shown by the short-dashed line in Fig. 7. At the range of radii from  $10^2 r_g$  to around  $10^4 r_g$  the short-dashed model is an ADAF, which is similar to the self-similar solution of Narayan & Yi (1995), where  $H/R \approx const$  and  $\Omega/\Omega_K \approx const$ . At  $r \gtrsim 10^5 r_g$  the radiative cooling becomes important in the energy balance and the solution ceases to be of the ADAF type. However, the end of the ADAF-type part for the other models shown in Figs 6 and 7 must be of a different nature. It cannot be connected to the cooling mechanisms, because both adiabatic and non-adiabatic models show very similar behaviour. One should note that the position of the end of the ADAF is determined by the value of the parameter  $r_s$ : a larger  $r_s$  corresponds a smaller transition radius.

The absence of the radially-unlimited ADAF solutions for  $\gamma_g = 5/3$  could be connected with the fact that there are no disc-like asymptotic self-similar solutions for  $\gamma_g = 5/3$ .

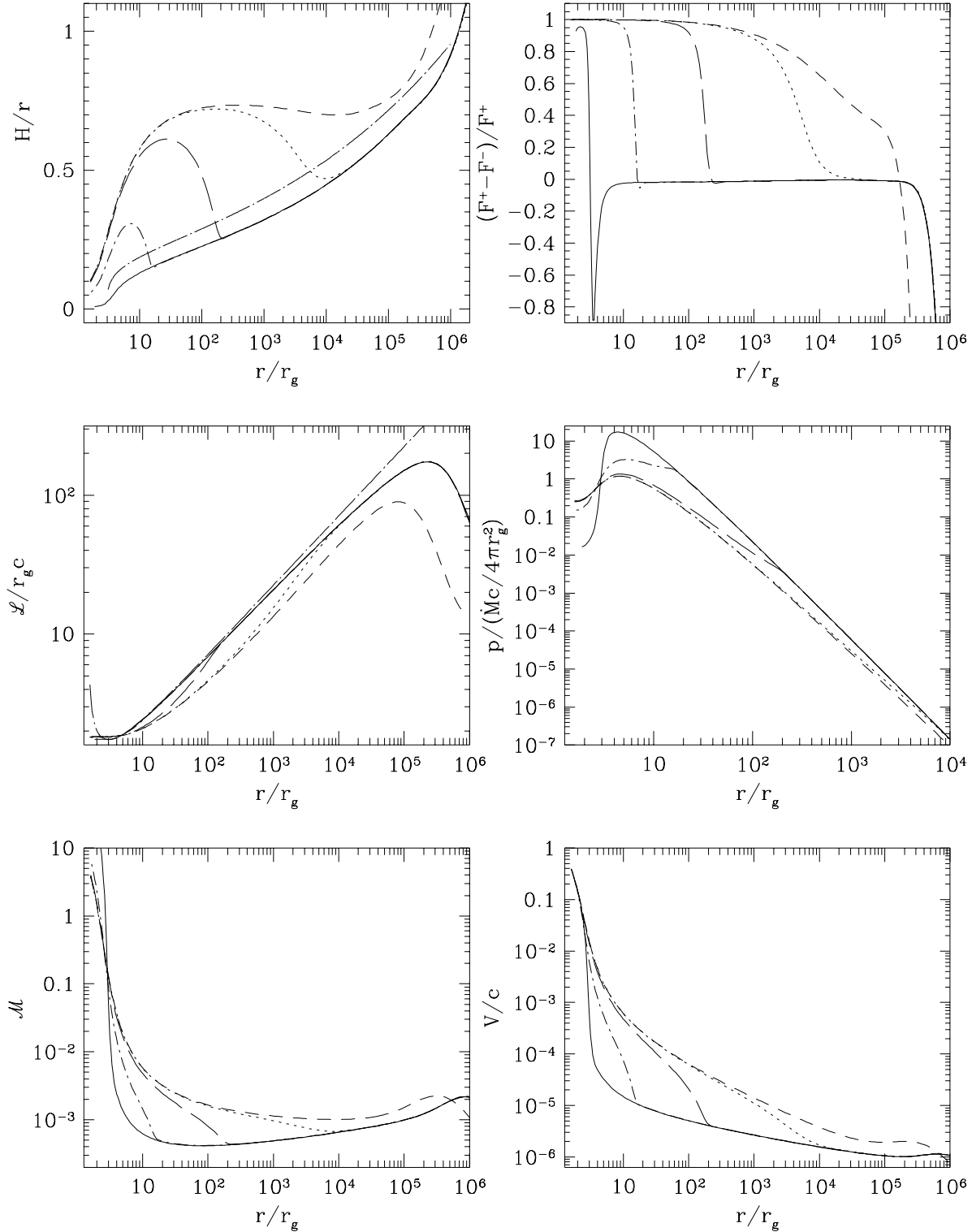


**Figure 7.** Selected properties of the bremsstrahlung models with  $\gamma_g = 4/3$ ,  $\alpha = 10^{-3}$ ,  $\dot{M}/\dot{M}_{Edd} = 10^{-5}$  and  $M = 10 M_\odot$ . Short-dashed, dotted, long-dashed, dotted-short-dashed and solid lines represent the cases  $r_s/r_g = 2.13075, 2.131, 2.14, 2.255$  and  $2.7$ , respectively. See the caption to Fig. 6 for further explanation.

The case  $\gamma_g = 5/3$  is singular (see Narayan & Yi 1995). On the other hand, we note, that the analogous self-similar solutions derived from the slim disc equations in the form given by Chen et al. (1997) are free from the  $\gamma_g = 5/3$  singularity. Our slim disc equations are similar to the ones

used by Narayan & Yi (1995), and therefore it is natural that our results agree with theirs. The question, however, remains of why different versions of the slim disc equations produce qualitatively different solutions at large radial distances  $r \gtrsim 10^2 r_g$ ? Are seemingly ‘formal’ details of the ver-

tical integration crucial for the physics of slim disks? Is the slim disc approach questionable in application to ADAFs? The best way to answer these questions would be by constructing fully two dimensional, non-stationary models of ADAFs.

There is a less important, but related, problem here. We have not obtained global solutions with shocks like those reported by Chakrabarti and collaborators (see Chakrabarti 1996) despite the very similar physics and boundary conditions assumed. Some of our solutions have transition regions which are narrow, but smooth with their inner structure being numerically well resolved. These narrow transitions are definitely *not* shocks. It is likely that this will be taken as an argument in the recent discussion ‘shocks or no shocks’ but we do not want to join in with this ourselves because we are convinced that the discussion is artificially inflated and of only academic interest. It does not touch a really interesting point here that one should be aware of. Several authors have recently studied general properties of transition regions between ADAFs and thin discs (see e.g. Regev, Lasota & Abramowicz 1997; Abramowicz et al. 1997b) and concluded that the physical conditions in the transition region are very complex, and cannot be described by any simple one-dimensional, stationary approach. Details of the vertical structure and dissipative processes are fundamental for the structure of the transition region and must be fully taken into account. Thus, one should first construct a more *physical* model of the transition region, before speculating about its nature.

## ACKNOWLEDGMENTS

We thank Kees Dullemond, Jean-Pierre Lasota, Roberto Turolla and Craig Wheeler for stimulating discussions. We thank John Miller for his helpful comments on the paper. This work was partially supported by the Swedish Natural Science Research Council, by Nordita’s Nordic Project *Non-linear phenomena in accretion discs around black holes*, by the Danish Natural Science Research Council through grant 11-9640-1, and by the Danish National Research Foundation through its establishment of the Theoretical Astrophysics Center.

## REFERENCES

- Abramowicz M. A., Calvani M., Nobili L., 1980, ApJ, 242, 772  
 Abramowicz M. A., Zurek W. H., 1981, ApJ, 246, 314  
 Abramowicz M. A., Czerny B., Lasota J. P., Szuszkiewicz E., 1988, ApJ, 332, 646 (ACLS88)  
 Abramowicz M. A., Chen X., Kato S., Lasota J. P., Regev O., 1995, ApJ, 438, L37  
 Abramowicz M. A., 1996, in *Physics of accretion discs*, eds Kato S., Inagaki S., Mineshige S. and Fukue J., Gordon and Breach science publishers, p. 1  
 Abramowicz M. A., Chen X.-M., Granath M., Lasota J.-P., 1996, ApJ, 471, 762 (ACGL96)  
 Abramowicz M. A., Lanza A., Percival M. J., 1997a, ApJ, in press  
 Abramowicz M. A., Igumenshchev I. V., Lasota J.-P., 1997b, MNRAS, in press  
 Beloborodov A. M., Abramowicz M. A., Novikov I. D., 1997, ApJ, in press  
 Bondi H., 1952, MNRAS, 112, 195

- Chakrabarti S. K., 1996, ApJ, 471, 237  
 Chen X., Abramowicz M. A., Lasota J. P., Narayan R., Yi I., 1995, ApJ, 443, L61  
 Chen X., Abramowicz M. A., Lasota J. P., 1997, ApJ, 476, 61  
 Honma F., 1996, in *Physics of accretion discs*, eds Kato S., Inagaki S., Mineshige S. and Fukue J., Gordon and Breach science publishers, p. 31  
 Jaroszyński M., Kupriewski A., 1997, A&A, in press  
 Lasota J.-P., 1994, in *Theory of Accretion Disks - 2*, eds W. J. Duschl, J. Frank, F. Meyer, E. Meyer-Hofmeister and W. M. Tscharnuter, Dordrecht: Kluwer, p. 341  
 Matsumoto R., Kato S., Fukue J., Okazaki A. T., 1984, PASJ, 36, 71  
 Muchotrzeb B., 1983, Acta Astron., 33, 79  
 Nakamura K., Kusunose M., Matsumoto R., Kato S., 1997, PASJ, in press  
 Narayan R., Yi I. 1994, ApJ, 428, L13  
 Narayan R., Yi I. 1995, ApJ, 444, 231  
 Narayan R., Kato S., Honma F. 1997, ApJ, 476, 49  
 Narayan R. 1997, in press (astro-ph/9611113)  
 Novikov I. D., Torn K. S., 1973, in *Black Holes*, eds. C. De Witt and B. S. De Witt, New York: Gordon and Breach, p. 343  
 Paczyński B., Wiita J., 1980, A & A, 88, 23  
 Paczyński B., Bisnovaty-Kogan G., 1981, Acta Astron., 31, 283  
 Piran T., 1978, ApJ, 221, 652  
 Press W. H., Teukolsky S. A., Vetterling W. T., Flannery B. P. 1992, *Numerical recipes in FORTRAN: the art of scientific computing*, Cambridge University Press, pp. 372, 753  
 Pringle J.E., Rees M.J. 1972, A&A, 21, 1  
 Regev O., Lasota J. P., Abramowicz M. A., 1997, in preparation  
 Shakura N. I., 1972, Soviet Astron., 16, 756  
 Shakura N. I., Sunyaev R. A. 1973, A&A, 24, 337  
 Shapiro S. L., Lightman A. P., Eardley D. M. 1976, ApJ, 204, 187 (SLE)

This paper has been produced using the Royal Astronomical Society/Blackwell Science L<sup>A</sup>T<sub>E</sub>X style file.